



RESEARCH ARTICLE

CHITOSAN COATED ROSUVASTATIN NANOSTRUCTURED LIPID CARRIERS: FORMULATION, IN VITRO CHARACTERIZATION AND STORAGE ASSESSMENTS

Walid Anwar^{*} , El Sayed Gamal E. Shaheen , Sherif K. Abu-Elyazid , Mohsen I. Afouna

Pharmaceutics Department, Faculty of Pharmacy, Al-Azhar University, Nasr City, Cairo, Egypt.

Article Info:

Abstract



Article History:

Received: 9 April 2025

Reviewed: 12 May 2025

Accepted: 22 June 2025

Published: 15 July 2025

Cite this article:

Anwar W, E. Shaheen ESGE, Abu-Elyazid SK, Afouna MI. Chitosan coated rosuvastatin nanostructured lipid carriers: Formulation, *in vitro* characterization and storage assessments. Universal Journal of Pharmaceutical Research 2025; 10(3): 28-35.

<http://doi.org/10.22270/ujpr.v10i3.1363>

*Address for Correspondence:

Dr. Walid Anwar, Pharmaceutics Department, Faculty of Pharmacy, Al-Azhar University, Nasr City, Cairo, Egypt. Tel: 00201066429953. E-mail: wawar8182@azhar.edu.eg

Background and Objective: Rosuvastatin calcium (ROS-Ca) is a synthetic, highly potent third-generation HMG-CoA reductase inhibitor with significant hypocholesterolemic effects. The objective of this study was to develop and characterize nanostructured lipid carriers (NLCs) as a delivery system for the poorly water-soluble drug rosuvastatin calcium (ROS-Ca), with the aim of enhancing its dissolution rate and improving oral bioavailability.

Methods: ROS-NLCs is prepared by hot homogenization-ultrasonication technique then the prepared formulations were further characterized. Finally compare their characteristics to the corresponding a positively charged chitosan coated to develop new CH-ROS-NLCs. In this study, glyceryl monostearate (GMS) was selected as solid lipids and Transcutol® HP as a liquid lipid, to develop ROS-NLC (nanostructured lipid carrier).

Results: The physicochemical properties were achieved. The prepared ROS-NLC formulation was showed in nanometric size (121.6±6.2 nm) with encapsulation efficiency (63±0.2%). Furthermore, ROS-NLC and CH-ROS-NLC appeared almost spherical nanoparticles in morphology under transmission electron microscope (TEM). DSC, XRD and FT-IR analysis showed that ROS was miscible, compatible, and incorporated into NLCs in amorphous form not in native crystalline state.

Conclusion: The previously results showed that ROS-Ca was successfully encapsulated into nanostructured lipid carriers (NLCs) which coated with chitosan CH-ROS-NLC to overcome the above-mentioned defects and, it was ensured that nanostructured lipid carriers have high beneficial effect for enhancing and improving the oral bioavailability of poorly water-soluble drugs such as Rosuvastatin.

Keywords: Glyceryl monostearate, hyperlipidemia, nanostructured lipid carriers, Rosuvastatin calcium.

INTRODUCTION

Rosuvastatin (ROS-Ca) is a synthetic, high potent third-generation statin with excellent cholesterol-lowering activity. ROS-Ca competitively inhibits hydroxymethylglutaryl-coenzyme A (HMG-CoA) reductase that catalyzes the conversion of HMG-CoA to mevalonic acid, the rate-limiting step in cholesterol biosynthesis, and thus, it is used for hyperlipidemia¹. ROS-Ca falls on bio pharmaceutical classification system (BCS) Class II (low solubility and high permeability), it is lipophilic (log p ~ 1.9) in nature and has an oral bioavailability of 20%^{2,3}. The low bioavailability of ROS-Ca is related to its poor aqueous solubility. In recent years, lipidic drug delivery systems have generated high hopes due to their beneficial

influence on drug absorption and bioavailability. Although (micelles), liposomes, and nano emulsions have been promising, lipid-based systems are susceptible to degradation in storage and by acidic environment in stomach and gastrointestinal tract (GIT) as well as GIT enzymes and bile salts⁴. In order to address these drawbacks, Muller *et al.*, thoroughly investigated biocompatible, biodegradable solid lipids and as a result SLNs were conceived in the early 1990s to overcome stability and toxicity limitations of classic lipid formulations. But the SLNs have disadvantages as low drug loading capacity and drug expulsion with time because these systems transformed from a higher energy state to more ordered one (β) upon storage⁵. In the early 2000s, researchers developed modified, second-generation nanostructured lipid carriers (NLCs)

to overcome the limitations of traditional solid lipid nanoparticles (SLNs), specifically aiming to improve drug loading capacity and stabilize their physical state³. NLCs are formulated by combining solid and liquid lipids, resulting in a less ordered internal structure. This unique arrangement allows for greater incorporation of drug molecules within the matrix, ultimately enhancing drug loading and stability throughout the product's shelf life⁶.

Numerous studies indicate that the heightened entrapment efficiency observed in NLCs stems from the structural differences between the two types of lipids incorporated solid and liquid. This irregularity generates imperfections within the lipid matrix, creating additional space to accommodate drug molecules. Upon solidification, this structural arrangement further facilitates drug loading. Additionally, the superior solubility of many drugs in liquid lipids, as opposed to solid lipids, contributes significantly to the overall entrapment capacity.

Alongside these advantages, NLCs are also recognized for their enhanced shelf stability, distinguishing them as a more advanced and effective drug delivery system when compared to conventional lipid-based carriers⁷.

NLCs are notable for their ability to encapsulate both hydrophilic and lipophilic drugs, offering considerable versatility in drug delivery. They don't just release drugs immediately; instead, they can provide a sustained release, which reduces dosing frequency and potentially improves patient compliance. Targeted delivery is another key advantage, as these systems can direct drugs more precisely to the intended site of action, minimizing off-target effects. Such attributes make NLCs especially promising for chronic disease management, where consistent therapeutic levels are crucial.

This review examines the composition and fabrication methods of NLCs, detailing their physicochemical properties and their utility as oral drug delivery vehicles. It also discusses recent advancements aimed at further enhancing their performance, particularly in improving the oral bioavailability of various pharmaceutical agents⁸. This study focused on developing nanostructured lipid carriers (NLCs) for the poorly water-soluble drug Rosuvastatin Ca (ROS-Ca), aiming to improve its oral bioavailability. After the initial preparation of ROS-NLCs, the formulations underwent surface modification using chitosan, a mucoadhesive polymer. Both coated and uncoated NLCs were then lyophilized to obtain dry powders. These powders were subsequently characterized by a range of analytical techniques, including DSC, XRD, FTIR, and *in vitro* release studies, to comprehensively evaluate their properties⁹. Finally, the shelf stability testing at room temperature (20°C) and refrigerator (4 °C) was carried out for 6 months¹⁰.

MATERIALS AND METHODS

Rosuvastatin calcium (ROS-Ca) was generously supplied by EIPICO, Cairo, Egypt. Transcutol® HP (highly purified diethylene glycol monoethyl ether)

was kindly provided as a gift sample from Gattefosse, France.

Glyceryl Mono Stearate (GMS), Poloxamer 188 (polyoxyethylene-polyoxypropylene (150:29) block copolymer), Tween®80 (polyoxyethylene (20) sorbitanmonooleate), chitosan, and methanol were all sourced from Sigma Aldrich, Inc., USA.

Fabrication of Nanostructured Lipid Carrier (NLC)

Building on the methodology described in previous studies^{11,12}, ROS-Ca nanostructured lipid carriers (ROS-NLCs) were formulated using a hot homogenization combined with ultrasonication, though several modifications were introduced. In summary, a predetermined amount of the selected solid-liquid binary lipid mixture (in a 70:30 ratio) was accurately weighed and then melted at a temperature 5°C above the melting point of the solid lipid¹³⁻¹⁵.

A known concentration of ROS-Ca (5% w/w relative to total lipids) was incorporated into the prepared oil phase, which itself consisted of a 5% (w/w) mixture of solid and liquid lipids. The aqueous phase, containing the selected surfactant, was heated to match the temperature of the oil phase. It was then gradually added drop wise to the oil phase under magnetic stirring at 1500 rpm for 10 minutes. Subsequently, the resulting pre-emulsion underwent homogenization using an Ultra-Turrax T25 homogenizer at 20,000 rpm for 15 minutes, as previously described by Nasirizadeh and Malaekheh-Nikouei⁸. The resultant o/w nano-emulsion was subjected to probe sonication at 60 % amplitude for 10 min. The obtained NLC dispersion was cooled down to room temperature.

Chitosan-Coated ROS-NLCs

Chitosan at 0.2% w/v was dissolved in 1% v/v aqueous acetic acid and allowed to stand overnight at pH 5.5. Subsequently, the NLC dispersion was introduced dropwise into the chitosan solution at a 1:1 ratio, while maintaining continuous stirring at 200 rpm for one hour to ensure thorough coating¹⁶⁻¹⁸.

The prepared chitosan-coated ROS-NLCs (CH-ROS-NLCs) were centrifuged using a cooling centrifuge (18,000 rpm, 15 min) and lyophilized using a cryoprotectant for further study⁹.

Freeze-drying study (Lyophilization)

The NLC dispersion underwent lyophilization to enhance long-term stability. Mannitol was incorporated at a concentration of 5% w/v to serve as a cryoprotectant. The prepared samples were initially frozen at -20°C for 24 hours, after which they were subjected to lyophilization for 36 hours¹⁶. Following the protocol, the lyophilized sample was reconstituted using PBS (pH 6.8) to prepare it for the upcoming experiments.

Characterization of ROS-NLCs

Particle size (PS), zeta potential (ZP) measurement and polydispersity index (PDI)

The particle size (PS) and polydispersity index (PDI) of the NLC were determined using dynamic light scattering on a Zetasizer instrument, which analyzes Brownian motion to assess particle size. The PDI provides an indication of the sample's homogeneity; lower PDI values suggest a more uniform particle distribution, while values above 0.5 reflect significant heterogeneity within the system⁸.

The average particle diameter and polydispersity index were determined using a Zetasizer Nano-ZS. This instrument utilizes a 10 mW He-Ne laser operating at a wavelength of 633 nm, with measurements taken at a back-scattering angle of 90° and a temperature of 25°C¹⁹. Zeta potential refers to the electrical potential present at the interface where the mobile dispersion medium meets the stationary layer of fluid adhering to a dispersed particle. This boundary essentially marks the transition between the bulk liquid and the immobilized region surrounding the particle, and measuring the zeta potential provides valuable insight into the stability and behavior of colloidal systems²⁰.

Zeta potential essentially reflects the electrostatic “personality” of particles in suspension, and it’s pretty central to understanding both their stability and surface properties. If these particles have a strong enough charge positive or negative they’ll generally repel each other and resist clumping, which is crucial for maintaining stable nanostructured lipid carriers (NLCs) over time. That’s why measuring zeta potential isn’t just some optional step; it’s genuinely useful for predicting whether your NLCs will stay dispersed or just form a sad, useless sludge.

To determine zeta potential in these NLC formulations, researchers used a Zetasizer Nano-ZS, which gauges how fast the particles move under an electric field (that’s the electrophoretic mobility bit). The Helmholtz–Smoluchowski equation was then used to actually calculate the zeta potential, and each measurement was repeated three times to ensure accuracy. For particle size, PDI (polydispersity index), and zeta potential measurements, the ROS-NLC samples had to be diluted first a 1:200 ratio with double-distilled water to get the right scattering intensity for photon correlation spectroscopy (PCS). All measurements were performed in triplicate, in line with standard reproducibility practices²¹.

Entrapment efficiency (EE) and drug loading (DL)

To assess entrapment efficiency and drug loading in the NLC formulations, 2 ml of the sample was subjected to ultracentrifugation at 100,000 rpm for one hour at 4°C. This process was conducted using a cooling ultracentrifuge to quantify the amount of untrapped ROS-Ca remaining in the supernatant¹⁹.

Following centrifugation, the supernatant was carefully collected and filtered through a 0.2 mm Millipore VR membrane. The filtrate was then diluted appropriately with methanol. Subsequent analysis was performed using a UV-Vis spectrophotometer at 244 nm to quantify the amount of unencapsulated drug. Based on these data, entrapment efficiency (% EE) and drug loading were calculated using standard equations-

$$\% EE = \frac{W_t - W_f}{W_t} \times 100$$

$$DL = \frac{W_t - W_f}{W_l} \times 100$$

Where, W_t was the total amount of ROS-Ca, W_f was the amount of unencapsulated drug and W_l was the weight of the lipid (solid+liquid lipid)^{9,22}.

Particle morphology

The morphology of the ROS-NLC particles was characterized by transmission electron microscopy

(TEM) to assess the surface features of the nanoparticles and to determine if any colloidal species, aside from the anticipated NLCs, were present. For sample preparation, the ROS-NLC dispersion was diluted at a 1:200 ratio with double-distilled water. A drop of this diluted sample was then placed onto film-coated copper grids and allowed to air-dry overnight at room temperature. The dried specimens were subsequently examined under TEM to visualize and analyze their microstructure²².

Degree of crystallinity and polymorphism

Differential scanning calorimetry (DSC) was utilized to analyze the thermal characteristics of the bulk excipients and to determine the crystallinity and possible polymorphic forms present in the NLC formulations. DSC thermograms were recorded for selected samples, including GMS solid lipid, both coated and uncoated ROS-NLC, blank NLCs (coated and uncoated), and ROS powder. Each sample, weighing a minimum of 3 mg, was sealed in aluminum pans and subjected to heating from 25 °C to 250 °C at a rate of 5 °C per minute. Key thermal parameters such as melting points, enthalpy changes, and onset temperatures of observed transitions were documented²²⁻²⁴.

Fourier transforms infrared spectroscopy (FT-IR)

To assess potential interactions between ROS and other components within the NLC, FT-IR analysis was conducted. Samples included residues from both coated and uncoated ROS-NLC, blank (drug-free) NLCs with and without coating, pure ROS powder, pure GMS powder, and a physical mixture of ROS and GMS. Each specimen underwent individual scanning within the 4000 to 650 cm^{-1} wave number range, at a resolution of 4 cm^{-1} , using the transmission mode on an FT-IR spectrometer^{25,26}.

X-ray diffraction analysis (XRD)

X-Ray diffraction analysis (XRD) was performed using X-Ray diffractometer to characterize the crystalline phases and detect the amorphous structure in the samples. The crystalline state of ROS-Ca was evaluated with X-ray powder diffraction. The X-ray generator was operated at 40 KV tube voltages and 40 mA of tube current, using the Ka lines of copper as the radiation source. The scanning angle ranged from 1 to 600 of 2θ in step scan mode²⁷.

In-vitro drug release

In this study, we evaluated the *in-vitro* release profiles for pure ROS, as well as for an equivalent dose (2.5 mg) from both the lyophilized, coated CH-ROS-NLC and the uncoated ROS-NLC formulations. Each sample was carefully weighed and sealed inside a dialysis bag (molecular weight cut-off: 12–14 kDa). The sealed bags were then placed in 250 mL of phosphate buffer (pH 6.8) containing 0.5% (w/w) Tween 20 to ensure adequate sink conditions. All flasks were incubated in a shaking water bath (Model 1031, GFL Corporation, Burgwedel, Germany) maintained at 37°C with a shaking speed of 100 rpm²⁸⁻³⁰.

The parameters of the *in vitro* release study were selected to achieve the sink condition. At each designated time point (0.5, 1, 2, 4, 6, 8, 10, 12, 18, 24, 36, and 48 hours), a 5 mL aliquot was withdrawn and

immediately replaced with an equal volume of fresh dissolution medium to maintain sink conditions. All collected samples were filtered using a 0.250 μm syringe filter prior to analysis³¹, the amount of ROS present in the collected samples was measured using a spectrophotometer at 244 nm. Each formulation was tested in triplicate, and the average values were calculated.

Storage stability study

A stability assessment of the prepared ROS-NLCs formulation was conducted over a six-month period. The nanodispersions were placed in securely sealed amber glass containers and kept at room temperature (approximately $25\pm 2^\circ\text{C}$, with 65% relative humidity) as well as in a refrigerated environment ($4\pm 2^\circ\text{C}$). The stored samples were visually inspected for any physical alterations such as aggregation or phase separation. Additionally, evaluations were carried out at intervals of one month, three months, and six months to check the average PS, PDI, and ZP³².

Statistical analysis

Data shown are the mean \pm SD and were analyzed by one-way ANOVA using Graph-Pad Prisme software version 6.07 (Graph Pad, San Diego, California); *p* values less than 0.05 were considered statistically significant.

RESULTS AND DISCUSSIONS

Fabrication of ROS nanostructured lipid carriers (NLCs)

The lipid phase utilized glycerylmonostearate (GMS) as the solid lipid and Transcutol® HP as the liquid lipid, both selected due to their demonstrated capacity to solubilize ROS-Ca effectively. For the aqueous phase, a combination of Poloxamer 188 and Tween 80 in a 1:1 ratio was employed as surfactants, reflecting

standard practice for enhancing stability and dispersion. The concentration of ROS-Ca was consistently maintained at 5% (w/w) relative to the lipid phase, and the total lipid content was restricted to no more than 5% (w/w) of the formulation. These methodological choices are in agreement with findings reported in previous studies^{8,33}, which was observed that increasing the lipid concentration resulted in noticeably larger particle sizes, which aligns with previous findings. Given that these formulations were designed for oral administration, the surfactant content was limited to a maximum of 2.5% (w/w). Details regarding the specific composition can be found in Table 1. The ROS-NLCs were prepared using a two-step process involving homogenization, followed by probe sonication.

Physicochemical characterization

The value of particle size, PDI, and zeta potential of prepared (CH-ROS-NLCs) was found to be 251.7 ± 2.3 nm, 0.43 ± 0.02 and 35.6 ± 2.3 mV respectively, while, (ROS-NLC) was observed to be 121.6 ± 6.2 nm, 0.36 ± 0.03 and -9.5 ± 3.7 mV respectively, Table (1).

Incorporation of chitosan during the preparation of NLCs led to the deposition of this cationic polymer onto the particle surfaces, resulting in an increased zeta potential and the formation of a thicker outer membrane. Consequently, the CH-ROS-NLCs formulations demonstrated a larger particle size compared to the corresponding ROS-NLCs. This observation aligns well with the particle size analysis data and is consistent with findings reported in previous studies^{2,16,17}. It was observed from Table 1 that the entrapment efficiency (EE) and loading capacity (LC) of CH-ROS-NLC and ROS-NLCs were 68 ± 0.3 , $3.40\pm 0.23\%$ and 63 ± 0.2 , $3.15\pm 0.16\%$, respectively.

Table 1: Composition and physicochemical characterization of ROS-NLCs.

Lipid phase		
Solid lipid 70% of lipids	GMS	
Liquid lipid 30% of lipids	Transcutol® HP	
Drug = 5% of total lipids (w/w)	ROS-Ca	
Aqueous phase		
Surfactants 2.5% (w/w) by ratio (1:1) water	Poloxamer 188: Tween 80	
Physicochemical characterization	ROS-NLC	CH-ROS-NLC
Particle size (PZ)	121.6 ± 6.2 nm	251.7 ± 2.3 nm
Poly dispersity index (PDI)	0.36 ± 0.03	0.43 ± 0.02
Zeta potential (ZP)	-9.5 ± 3.7 mV	35.6 ± 2.3 mV
Encapsulation efficiency (EE)	$63\pm 0.2\%$	$68\pm 0.3\%$
Loading capacity (LC)	$3.15\pm 0.16\%$	$3.40\pm 0.23\%$

Transmission Electron Microscopy (TEM)

The surface morphology and mean particle diameter of the prepared nanostructured lipid carrier (NLC) formulations were characterized using transmission electron microscopy (TEM). TEM analysis revealed nearly spherical nanoparticles with a monodisperse size distribution below 200 nm, indicating uniform particle dispersion and minimal aggregation. Both uncoated NLCs and chitosan-coated NLCs (CH-NLCs) exhibited spherical morphology, with CH-

NLCs displaying a distinct outer polymeric shell. The incorporation of chitosan (CH) during NLC synthesis facilitated the electrostatic deposition of this cationic polysaccharide onto the particle surface, forming a dense polymeric coating. Furthermore, CH-NLCs demonstrated a larger hydrodynamic diameter compared to their uncoated counterparts, consistent with the presence of the CH outer layer as showed in Figure 1. This findings with the same line of other study^{2,8,9}.

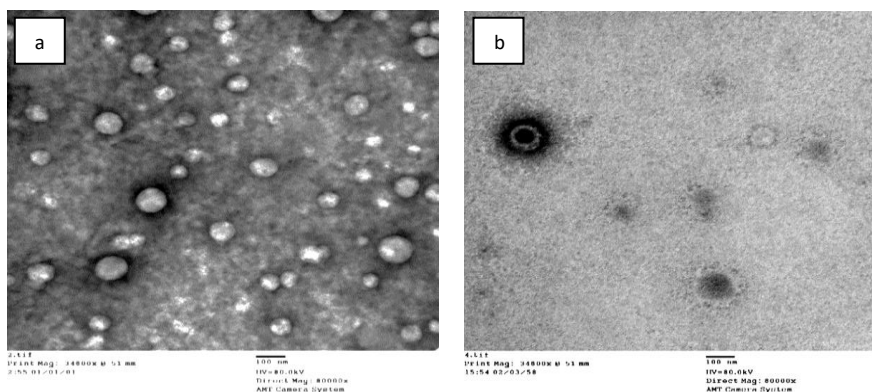


Figure 1: TEM images of ROS-NLC (a) and CH-ROS-NLC (b).

Fourier Transform Infrared spectroscopy analysis

FT-IR analysis was conducted to confirm the absence of any physical or chemical interactions between pure ROS-Ca and the other NLC excipients. Figure 2 demonstrate the IR spectrum of ROS-Ca showed distinct peaks corresponding to the primary functional groups: OH, in the carboxylic group around 1547 cm⁻¹, Hydroxyl groups between 3400-3700 cm⁻¹, Olefinic C-H of the heptanoic side chain near 2922 cm⁻¹ and Sulphoxide group approximately at 1330 and 1381 cm⁻¹. The IR spectrum of GMS displayed a band for the C=O of an ester around 1735 cm⁻¹ and bands for C-H aliphatic stretching approximately between 2800-2900 cm⁻¹. Fourier-transform infrared (FTIR) spectroscopy analysis of the rosuvastatin calcium-loaded nano-structured lipid carriers (ROS-NLCs) confirmed the absence of drug-excipients interactions, as evidenced by the preservation of all characteristic functional group absorption bands of ROS-Ca at their respective wave numbers, identical to those observed in the spectrum of pure ROS-Ca. The lack of peak shifts or band disappearance in the ROS-NLCs spectrum suggests no significant physico-chemical interactions between the drug and the lipid matrix/excipients. Furthermore, the spectral similarity between blank NLCs and ROS-NLCs reinforces the conclusion that ROS-Ca remains molecularly intact without forming new bonds or undergoing degradation within the formulation²⁴. These findings align with previously reported studies on similar lipid-based nanocarrier systems^{34,35}.

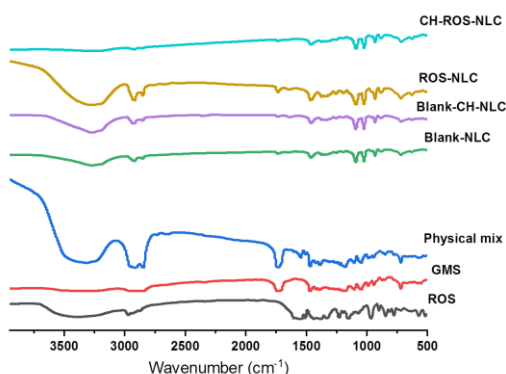


Figure 2: FT-IR spectra of ROS, GMS, physical mixture, Blank-NLC, Blank-CH-NLC, ROS-NLC and CH-RO-NLC.

Differential scanning Calorimetry (DSC)

Assessing the crystallinity of NLCs is crucial as it affects both encapsulation efficiency and drug release. To obtain data on the crystallinity of the NLCs and the interactions between the drug and lipids within the formulation, DSC analyses were conducted.

DSC thermograph of pure ROS-Ca showed a sharp endothermic peak at 144°C which corresponds to its melting point Figure 3. DSC thermograph of GMS showed a sharp endothermic peak at 65°C which corresponded to its melting point. DSC thermograph of the lyophilized powder of Blank, CH-ROS-NLCs and ROS-NLCs showed a sharp endothermic peak at 165.8°C owing to the presence of mannitol as cryoprotectant²⁸.

The Blank, CH-ROS-NLC, and ROS-NLC formulations exhibited a minor temperature shift for GMS. This phenomenon could be due to their nanoparticle size, lipid phase dispersion, and the presence of certain excipients like surfactants^{1,36}.

The ROS-NLC formulations lacked the typical endothermic peak associated with the drug, indicating that the drug is fully incorporated or molecularly dispersed in an amorphous form within the solid matrix, as illustrated in Figure 3.

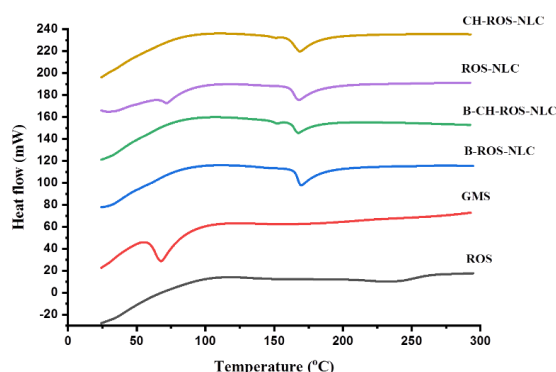


Figure 3: DSC thermograms of ROS, GMS, B-ROS-NLC, B-CH-ROS-NLC, ROS-NLC and CH-ROS-NLC.

X-Ray Diffraction analysis (XRD)

The XRD study was performed with support of DSC to distinguish the reduction in crystalline nature of ROS-Ca in prepared NLCs. The XRD spectra of ROS-Ca, GMS and the physical mixture in Figure 4 display prominent and sharp peaks at the 2θ scale, signifying

the crystalline structure of the drug. Conversely, the XRD pattern of ROS-NLCs in the same figure exhibits a marked reduction in the intensity of all peaks. This indicates that the ROS-Ca drug exists in a completely amorphous state within the NLC formulations^{22,37}. X-ray Diffractogram of ROS-Ca, GMS, physical mixture, CH-ROS-NLC, ROS-NLC, were illustrated in Figure 4 and showed that no interference between drug and other excipients.

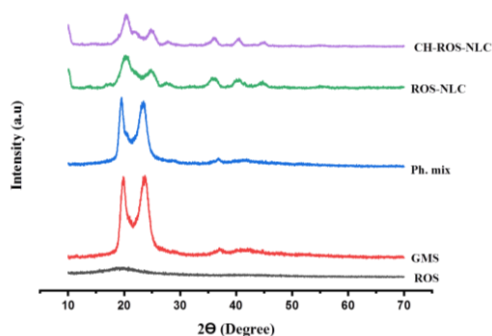


Figure 4: XRD spectra of ROS, GMS, PH. MIX, ROS-NLC, and CH-ROS-NLC.

***In-vitro* drug release**

The ROS-loaded nanostructured lipid carriers (ROS-NLC) and chitosan-coated ROS-NLCs (CH-ROS-NLCs) exhibited an initial burst release of $14.7 \pm 3.9\%$ and $10.3 \pm 2.7\%$, respectively, in PBS (pH 6.8) (Figure 4). Subsequently, a sustained and gradual release was observed, reaching $69.9 \pm 6.6\%$ for ROS-NLCs and $58.4 \pm 3.7\%$ for CH-ROS-NLCs after 24 hours. In contrast, free ROS displayed a much faster release; with $84.1 \pm 2.7\%$ of the drug being released within the first hour (Figure 5). Indicating that ROS-NLCs release the drug at a faster rate than CH-ROS-NLCs over the same period². The slower and more controlled release from CH-ROS-NLCs can be attributed to the chitosan (CH) coating, which acts as a diffusion barrier, delaying the release of the entrapped ROS³⁸. On the other hand, the relatively faster release from ROS-NLCs may be due

to incomplete drug retention within the lipid matrix, leading to quicker diffusion.

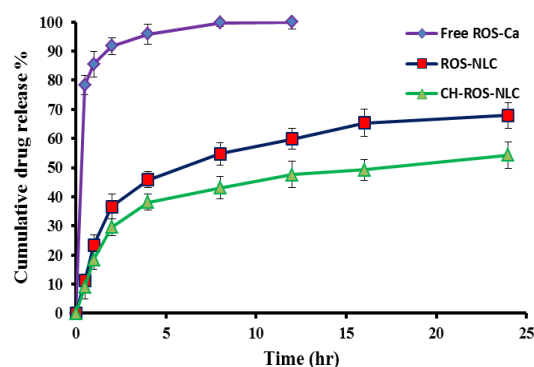


Figure 5: Cumulative release % profile of Rosuvastatin (ROS).

Effect of storage condition on Optimized ROS-NLCs

Effect of storage was conducted for the prepared formulations CH-ROS-NLC (F1) and ROS-NLC (F2) at room temperature (approximately $25 \pm 2^\circ\text{C}$) and in a refrigerator (approximately $4 \pm 2^\circ\text{C}$) for six months. Measurements of particle size, polydispersity index, and zeta potential are detailed in Table 2. Upon initial visual inspection, no signs of agglomeration or phase separation were observed throughout the study period. After three months of storage at room temperature, the results showed an increase in both particle size and polydispersity index, while zeta potential values decreased compared to the freshly prepared samples. These findings indicate a reduction in colloidal stability over time. Conversely, only insignificant changes in mean particle size, polydispersity index, and zeta potential were observed when the formulas were stored in the refrigerator. These findings suggest that 4°C is the optimal storage temperature for NLCs. The negligible changes in the parameters can be attributed to minor polymorphic transitions of the lipid from the less stable α polymorph to the more stable β polymorph³⁹.

Table 2: Effect of storage conditions on coated and uncoated ROS-NLC formulations (F1 and F2).

F. N.	Storage condition	PS (nm)	PDI	ZP (mV)	Visual observation
Refrigerator (4°C)					
F1	Fresh	251.7 ± 2.3	0.43 ± 0.02	35.6 ± 2.3	Clear emulsion
	1 month	253.6 ± 2.5	0.44 ± 0.02	34.4 ± 2.2	Clear emulsion
	3 months	259.5 ± 2.6	0.44 ± 0.03	33.5 ± 2.5	Clear emulsion
	6 months	285.7 ± 3.5	0.46 ± 0.03	32.6 ± 2.6	Turbid emulsion
F2	Fresh	126.4 ± 2.6	0.36 ± 0.03	-9.5 ± 3.7	Clear emulsion
	1 month	130.6 ± 2.5	0.37 ± 0.02	-10.6 ± 2.3	Clear emulsion
	3 months	152.5 ± 2.3	0.37 ± 0.02	-10.5 ± 2.4	Clear emulsion
	6 months	185.5 ± 2.7	0.38 ± 0.03	-9.6 ± 2.2	Turbid emulsion
Room temperature (25°C)					
F1	Fresh	251.7 ± 2.3	0.43 ± 0.02	35.6 ± 2.3	Clear emulsion
	1 month	257.6 ± 2.5	0.44 ± 0.02	34.4 ± 2.2	Clear emulsion
	3 months	298.5 ± 3.6	0.46 ± 0.02	31.5 ± 2.5	Gelation, particulate
	6 months	418.7 ± 4.5	0.47 ± 0.03	30.6 ± 2.6	Gelation, particulate
F2	Fresh	126.4 ± 2.6	0.36 ± 0.03	-9.5 ± 3.7	Clear emulsion
	1 month	135.8 ± 2.5	0.37 ± 0.02	-8.7 ± 2.4	Clear emulsion
	3 months	187.5 ± 2.7	0.39 ± 0.02	-8.2 ± 2.1	Gelation, particulate
	6 months	265.5 ± 3.8	0.41 ± 0.03	-9.3 ± 2.4	Gelation, particulate

Limitations of the study

There is need of future studies to investigate the *in-vivo* pharmacokinetic profile of release of ROS and characterize both qualitative and quantitative aspects of particular cellular uptake and their subsequent impact on disease through pharmacodynamic examination in the presence and absence of chitosan coating.

CONCLUSIONS

This study establishes nanostructured lipid carriers (NLCs) as a promising oral drug delivery platform for rosuvastatin (ROS) in the treatment of hyperlipidemia. Through formulation, characterization both ROS-loaded NLC (ROS-NLC) and chitosan coated ROS-NLC (CH-ROS-NLC) exhibited superior physico-chemical stability, sustained drug release. The chitosan functionalized NLCs demonstrated augmented muco-adhesive properties, overcoming a major biopharmaceutical limitation in ROS delivery. Collectively, these findings position ROS-NLC and CH-ROS-NLC as nanotherapeutic strategies for treatment of hyperlipidemia through improving drug solubility and stability.

ACKNOWLEDGEMENT

The authors express gratitude to Pharmaceutics Department, Faculty of Pharmacy, Al-Azhar University, Nasr City, Cairo, Egypt to provide necessary facilities for this work.

AUTHOR'S CONTRIBUTION

Anwar W: Conceptualization, methodology, formal analysis, project administration, writing-review, editing, methodology, resources. **Shaheen ESGE:** Methodology. **Abu-Elyazid SK:** Investigation, software. **Afouna MI:** Supervision, editing. Final manuscript was checked and approved by all authors.

DATA AVAILABILITY

Data will be made available on request.

CONFLICT OF INTEREST

None to declare.

REFERENCES

- Rizwanullah, M, Amin S, Ahmad J. Improved pharmacokinetics and antihyperlipidemic efficacy of rosuvastatin-loaded nanostructured lipid carriers. *J Drug Target* 2017; 25:58–74. <https://doi.org/10.1080/1061186X.2016.1191080>
- Ahmed TA. Development of rosuvastatin flexible lipid-based nanoparticles: Promising nanocarriers for improving intestinal cells cytotoxicity. *BMC Pharmacol Toxicol* 2020;21. <https://doi.org/10.1186/s40360-020-0393-8>
- Shaheen, ESGE, Anwar W, Abu-Elyazid SK, Afouna, MI. Development, screening and optimization of rosuvastatin loaded nanostructured lipid carriers for improved therapeutic efficacy. *Universal J Pharm Res* 2024 2024; 9(5): 82-90. <https://doi.org/10.22270/ujpr.v9i5.1212>
- Beloqui A, Solinís MA, Rodríguez-Gascón A, *et al.* Nanostructured lipid carriers: Promising drug delivery systems for future clinics. *Nanomed: Nanotech Bio Med* 2016; 1:143–161. <https://doi.org/10.1016/j.nano.2015.09.004>
- Khan S, Sharma A, Jain V. An overview of nanostructured lipid carriers and its application in drug delivery through different routes. *Adv Pharm Bull* 2023;13:446–460. <https://doi.org/10.34172/apb.2023.056>
- Khan S, Baboota S, Ali J, *et al.* Nanostructured lipid carriers: An emerging platform for improving oral bioavailability of lipophilic drugs. *Int J Pharm Invest* 2015;5:182. <https://doi.org/10.4103/2230-973X.167661>
- Tang CH, Chen HL, Dong JR. Solid lipid nanoparticles (SLNs) and nanostructured lipid carriers (NLCs) as food-grade nanovehicles for hydrophobic nutraceuticals or bioactives. *Appl Sci* 2023;13:1726. <https://doi.org/10.3390/app13031726>
- Anwar W, Dawaba HM, Afouna MI, *et al.* Screening study for formulation variables in preparation and characterization of Candesartan cilexetil loaded nanostructured lipid carriers. *Universal J Pharm Res* 20202019; 4(6):8-19. <https://doi.org/10.22270/ujpr.v4i6.330>
- Anwar W, Kaseem AM, Salama A, *et al.* Optimisation of albendazole delivery and assessment of anticancer potential in hepatocellular carcinoma (HepG2 cells) using surface modified nanostructured lipid carriers. *J Microencapsul* 2025;42:161–176. <https://doi.org/10.1080/02652048.2025.2451848>
- Anwar W, Dawaba HM, Afouna MI, *et al.* Enhancing the oral bioavailability of Candesartan cilexetil loaded nanostructured lipid carriers: *In-vitro* characterization and absorption in rats after oral administration. *Pharmaceutics* 2020;12:1–19. <https://doi.org/10.3390/pharmaceutics12111047>
- Anwar W, Dawaba HM, Afouna MI, *et al.* Screening study for formulation variables in preparation and characterization of Candesartan cilexetil loaded nanostructured lipid carriers. *Universal J Pharm Res* 2019; 4:8–19. <https://doi.org/10.22270/ujpr.v4i6.330>
- Nnamani PO, Hansen S, Windbergs M, *et al.* Development of artemether-loaded nanostructured lipid carrier (NLC) formulation for topical application. *Int J Pharm* 2014; 477:208–217. <https://doi.org/10.1016/j.ijpharm.2014.10.004>
- Karimi KN, Radi M, Amiri S, *et al.* Fabrication and characterization of alginate-based films functionalized with nanostructured lipid carriers. *Int J Biol Macromol* 2021; 182:373–384. <https://doi.org/10.1016/j.ijbiomac.2021.03.159>
- Mathur P, Sharma S, Rawal S, *et al.* Fabrication, optimization, and *in-vitro* evaluation of docetaxel-loaded nanostructured lipid carriers for improved anticancer activity. *J Liposome Res* 2020; 30:182–196. <https://doi.org/10.1080/08982104.2019.1614055>
- Nasirizadeh S, Malaekheh-Nikouei B. Solid lipid nanoparticles and nanostructured lipid carriers in oral cancer drug delivery. *J Drug Deli Sci Tech* 2020;55. <https://doi.org/10.1016/j.jddst.2019.101458>
- Zafar A, Alruwaili NK, Imam SS, *et al.* Formulation of chitosan-coated piperine NLCS: Optimization, *in-vitro* characterization, and *in-vivo* preclinical assessment. *AAPS Pharm Sci Tech* 2021;22. <https://doi.org/10.1208/s12249-021-02098-4>
- Bashiri S, Ghanbarzadeh B, Ayaseh A, *et al.* Preparation and characterization of chitosan-coated nanostructured lipid carriers (CH-NLC) containing cinnamon essential oil for enriching milk and anti-oxidant activity. *LWT* 2020; 119. <https://doi.org/10.1016/j.lwt.2019.108836>
- Nerli G, Goncalves LMD, Cirri M, *et al.* Design, evaluation and comparison of nanostructured lipid carriers and chitosan nanoparticles as carriers of poorly soluble

- drugs to develop oral liquid formulations suitable for pediatric use. *Pharmaceutics* 2023;15:1305.
<https://doi.org/10.3390/pharmaceutics15041305>
19. Krambeck K, Silva V, Silva R, et al. Design and characterization of nanostructured lipid carriers (NLC) and nanostructured lipid carrier-based hydrogels containing *Passiflora edulis* seeds oil. *Int J Pharm* 2021; 600:20444.
<https://doi.org/10.1016/j.ijpharm.2021>
 20. Rita OMP, Reis S, Nunes C, et al. Amoxicillin-loaded lipid nanoparticles against *Helicobacter pylori* infections 2016.
 21. Saghafi Z, Mohammadi M, Mahboobian MM, et al. Preparation, characterization, and *in-vivo* evaluation of perphenazine-loaded nanostructured lipid carriers for oral bioavailability improvement. *Drug Dev Ind Pharm* 2021; 47:509–520.
<https://doi.org/10.1080/03639045.2021.1892745>
 22. Chaudhari VS, Murty US, Banerjee S. Nanostructured lipid carriers as a strategy for encapsulation of active plant constituents: Formulation and *in-vitro* physicochemical characterizations. *Chem Phys Lipids* 2021;235:105037.
<https://doi.org/10.1016/j.chemphyslip.2020.105037>
 23. Yuan H, Wang LL, Du YZ, et al. Preparation and characteristics of nanostructured lipid carriers for control-releasing progesterone by melt-emulsification. *Colloids Surf B Biointerfaces* 2007;60:174–179.
<https://doi.org/10.1016/j.colsurfb.2007.06.011>
 24. Sivaraman G, Ponnuraj R, Özt AA. Formulation and characterization of rosuvastatin calcium nanoparticles related papers formulat ion and charact erizat ion of epigallocat echin gallat e nanopart icles clarit hromycin-loaded poly (LACT IC-co-glycolic acid) (PLGA). *Nanopart Icles for Oral Administ Rat Ion: Eff* 2015.
 25. Akbari J, Saeedi M, Ahmadi F, et al. Solid lipid nanoparticles and nanostructured lipid carriers: A review of the methods of manufacture and routes of administration. *Pharm Dev Tech* 2022;27:525–544.
<https://doi.org/10.1080/10837450.2022.2084554>
 26. Elmowafy M, Al-Sanea MM. Nanostructured lipid carriers (NLCs) as drug delivery platform: Advances in formulation and delivery strategies. *Saudi Pharma J* 2021; 29:999–1012.
<https://doi.org/10.1016/j.jsps.2021.07.015>
 27. Dolatabadi S, Karimi M, Nasirizadeh S, et al. Preparation, characterization and *in-vivo* pharmacokinetic evaluation of curcuminoids-loaded solid lipid nanoparticles (SLNs) and nanostructured lipid carriers (NLCs). *J Drug Deliv Sci Technol* 2021; 62:102352.
<https://doi.org/10.1016/j.jddst.2021.102352>
 28. Rizwanullah MD, Amin S, Ahmad J. Improved pharmacokinetics and antihyperlipidemic efficacy of rosuvastatin-loaded nanostructured lipid carriers. *J Drug Target* 2017; 25:58–74.
<https://doi.org/10.1080/1061186X.2016.1191080>
 29. Li J, Yang M, Xu W. Development of novel rosuvastatin nanostructured lipid carriers for oral delivery in an animal model. *Drug Des Dev Ther* 2018;12:2241–2248.
<https://doi.org/10.2147/DDDT.S169522>
 30. Ahmed TA. Development of rosuvastatin flexible lipid-based nanoparticles: Promising nanocarriers for improving intestinal cells cytotoxicity. *BMC Pharmacol Toxicol* 2020;21:14.
<https://doi.org/10.1186/s40360-020-0393-8>
 31. Parameswaran S, Ramamoorthy VG, Venkateswarlu VS, et al. Design, 23 factorial optimization and *in-vitro in-vivo* pharmacokinetic evaluation of rosuvastatin calcium loaded polymeric nanoparticles. *Inter J Appl Pharma* 2022:200–205.
<https://doi.org/10.22159/ijap.2022v14i2.43459>
 32. Gomaa E, Fathi HA, Eissa NG, et al. Methods for preparation of nanostructured lipid carriers. *Methods* 2022;199:3–8.
<https://doi.org/10.1016/j.jymeth.2021.05.003>
 33. Elbahwy IA, Ibrahim HM, Ismael HR, et al. Enhancing bioavailability and controlling the release of glibenclamide from optimized solid lipid nanoparticles. *J Drug Deliv Sci Technol* 2017;38:78–89.
<https://doi.org/10.1016/j.jddst.2017.02.001>
 34. Ghanem HA, Nasr AM, Hassan TH, et al. Comprehensive study of atorvastatin nanostructured lipid carriers through multivariate conceptualization and optimization. *Pharmaceutics* 2021; 13 (2): 178.
<https://doi.org/10.3390/pharmaceutics13020178>
 35. Hassan DH, Shohdy JN, El-Setouhy DA, El-Nabarawi M, Naguib MJ. Compritol-based nanostructured lipid carriers (nlcs) for augmentation of zolmitriptan bioavailability via the transdermal route: *in vitro* optimization, *ex vivo* permeation, *in vivo* pharmacokinetic study. *Pharmaceutics* 2022; 14 (7): 1484.
<https://doi.org/10.3390/pharmaceutics14071484>
 36. Gadad AP, Tigadi SG, Dandagi PM, Mastiholmath VS, Bolmal UB. Rosuvastatin loaded nanostructured lipid carrier: for enhancement of oral bioavailability. *Indian J Pharm Educ Res* 2016; 50:4.
<https://doi.org/10.5530/ijper.50.4.13>
 37. Shete MB, Deshpande AS, Shende PK. Nanostructured lipid carrier-loaded metformin hydrochloride: design, optimization, characterization, assessment of cytotoxicity and ROS evaluation. *Chem Phys Lipids* 2023; 250: 105256.
<https://doi.org/10.1016/j.chemphyslip.2022.105256>
 38. Farhadi M, Haniloo A, Rostamizadeh K, et al. *In-vitro* evaluation of albendazole-loaded nanostructured lipid carriers on *Echinococcus granulosus* microcysts and their prophylactic efficacy on experimental secondary hydatidosis. *Parasitol Res* 2021; 120:4049-4060.
<https://doi.org/10.1007/s00436-021-07343-0>
 39. Alshora DH, Ibrahim MA, Elzayat E, Almeanazel OT, Alanazi F. Rosuvastatin calcium nanoparticles: Improving bioavailability by formulation and stabilization codesign. *PLoS One* 2018; 13: 7.
<https://doi.org/10.1371/journal.pone.0200218>